Minerals Engineering 168 (2021) 106905

Contents lists available at ScienceDirect

Minerals Engineering

journal homepage: www.elsevier.com/locate/mineng

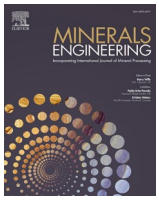

The double wheel breakage test

Marcos Bueno [a,*], Janne Torvela [b], Rajiv Chandramohan [c], Tabatha Chavez Matus [a], Toni Liedes [b], Malcolm Powell [d]

[a] Oulu Mining School, University of Oulu, P.O. Box 3000, FIN-90014 University of Oulu, Finland
[b] Mechatronics and Machine Diagnostics, University of Oulu, P.O. Box 3000, FIN-90014 University of Oulu, Finland
[c] Ausenco, 855 Homer St, Vancouver, BC V6B 2W2, Canada
[d] JKMRC, University of Queensland, 40 Isles Rd, Indooroopilly, QLD 4068, Australia

ARTICLE INFO

Keywords:
Geometallurgy
Comminution
Ore breakage characterization
Variability

ABSTRACT

The mining industry needs a low-cost and reliable breakage characterization test which can rapidly process a large number of samples for geometallurgical modelling. The more samples are tested, the better is the understanding of the ore hardness variability and lower the design or production risks. The proposed solution is a new testing device, herein named Geopyörä, which is a variation of a roll crusher with an adjustable gap and instrumentation to measure breakage forces and energy applied to rock particles during the breakage process. The principle utilises a controlled degree of crushing, with absorbed breakage energy being a response rather than an input. The new testing device is capable of rapidly testing rocks over a wide range of sizes and accurately measured energy levels. For a range of ores, the results were demonstrated to provide outputs that replicate the breakage modelling from full JK drop Weight tests. In addition to being suited to testing drill cores and small sample masses, the Geopyörä provides a distribution of particle strengths within every sample. This paper provides an introduction to the concept, development of the prototype device and breakage calibration results that indicate its potential to become a major player in geometallurgical ore testing.

1. Introduction

"What are the chances of achieving design capacity throughout the life of mining project?" Armed with answers to this question, one could take a lot of guesswork out of decision-making in mill design and plan strategies with more confidence. There are two main root causes of faults in mill designs: the selection of wrong design criteria and the use of poor design methodologies or inaccurate models. The selection of wrong design criteria occurs mainly due to lack of quality test work or misinterpretation of results and orebody variability (Bueno et al., 2015). A new prototype device named Geopyörä was built as a part of a project to develop a fast, low-cost, and reliable breakage characterization test for aiding geo-metallurgical modelling.

Commonly used comminution tests may be categorized broadly into three groups according to the type and mechanism of breakage. The first group of rock mechanical tests are characterized by applying slowly increasing forces until breakage is observed. The second group of particle breakage tests employs dynamic impact forces to break the sample. The third group of grindability tests measures the energy consumed in a rotating mill. The comminution behaviour is dependent on the amount, type, and rate of stresses applied to the material, as well as the dimensions and shape of the particles being tested. Therefore, different tests are used in different minerals processing contexts. The amount of sample materials in presently used tests range between 5 and 300 kg for small scale comminution testing, reaching up to tons for pilot scale plant operation (Mwanga et al., 2015, Chandramohan et al., 2015, Zhang, 2004, Grady & Lipkin, 1980).

A short selection of single particle impact type testing equipment comparable to the Geopyörä test includes the JK Drop Weight Test (JKDWT) (Napier-Munn et al., 1996), the Steve Morrell Comminution test (SMC) (Morrell, 2004), the Ultra-fast Load Cell Device (UFLC) (Weichert & Herbst, 1986), the Twin Pendulum test (Narayanan & Whiten, 1988), and the Split Hopkinson Bar test (SHBT) (Bourgeois, 1992). The basic operating principle of the DWT, the SMC, and the UFLC devices involves a heavy weight falling from a set height onto the sample particle, while the Twin Pendulum test uses a pair of freely swinging hammers set to crush a particle between their faces. The SHBT shoots a heavy steel projectile out of a pneumatic cannon to strike an assembly of

* Corresponding author.
E-mail address: geopyora@gmail.com (M. Bueno).

https://doi.org/10.1016/j.mineng.2021.106905
Received 8 June 2020; Received in revised form 8 March 2021; Accepted 6 April 2021
Available online 27 April 2021

two steel rods with the sample suspended in between. Various instrumented versions of the actual crushing equipment may also be used for the same purposes, although they are mostly intended for pilot scale operation and studying the forces applying to the crushing equipment itself, or they do not have the instrumentation for properly distinguishing the comminution energy of individual particles (Refahi et al., 2010, Lieberwirth et al., 2017, Nogychi & Watanabe, 1992, Morris, 1994).

The use of these tests generally involves correlating the applied breakage energy to the obtained amount of breakage to calculate a specific energy consumption, typically expressed in kilowatt-hours per ton (kWh/t). When the resulting rock fragments are sifted, the percentage of finer fragments t_n passing through a sieve grid $1/n$ the size of the original particle can be related to the specific energy by the mathematical function presented in Eq. (1). The parameters A and b are empirically obtained by fitting the curve to measurements while the applied energy level E is varied to produce the data. A fraction of 1/10 or t_{10} is commonly used (Napier-Munn et al., 1996).

$$t_n = A.(1 - e^{-b.Ecs}) \quad (1)$$

An obvious shortcoming in the various tests with falling weights is the application of nominal amounts of energy to the sample with the assumption that all the input energy is spent on comminution rather than secondary effects such as fragmented particles flying off, and varying re-breakage of the pieces still remaining under the dropped weight. In contrast, the Geopyörä test attempts to apply only as much energy as is needed to break the sample particle.

2. Geopyörä breakage test concept

The concept of this breakage test is to use counter-rotating wheels to nip and crush a rock with a tightly controlled reduction ratio from the feed to a defined gap between rollers, as illustrated in Fig. 1. This allows the automated feeding of rocks one at a time through the spinning wheels, with no requirement of stopping, resetting and sweeping away broken fragments between each rock breakage. It also allows to measure the force applied and energy consumed in each breakage event. The force applied to break a rock with a given degree of compression is a function of the rock compressive strength. In contrast to drop weigh test (DWT) methods, the input energy is a response to this crushing force, not a controlled test input. However, by varying the degree of reduction, that is the ratio of the crushing gap to the particle diameter, a range of input energies can be achieved for mapping the response of the rock to input force and the resultant input energy. In such a design it is necessary to measure the absorbed energy per rock breakage with sufficient precision, while ensuring non-slip grip and compression of the rocks to the point of fracture.

A prototype device as shown in Fig. 2 was design and built to fit this concept and allow accurate measurements of the absorbed energy in single particle breakage tests. The principle utilised by Lieberwirth et al., (2017) of rapidly decoupling the drive system was further refined using gearless motors and allowing the wheels to spin freely during breakage, with the energy being measured form the reduction in angular momentum of the wheels. The amount of comminution is varied by the opening of the wheel gap rather than setting a nominal applied impact energy. Since the particle sizes and shapes, as well as their individual properties are variable, this results in a distribution of values with a corresponding quantity of breakage products that represent the characteristics of the ore body from which the samples were obtained.

3. Mechanical design

A breakage testing device can be a purely mechanical system, such as a falling hammer or a dropping weight. When such tools or devices are augmented with intelligent automation, they become what is known as mechatronic systems (Acar & Parkin, 1996, Hsu, 1997). The device becomes an appliance that works to save time and labor for the technician and the researcher. The use of mechatronic engineering in designing such appliances means integrating basic machine design with electronic sensing and computational technology (Cetinkunt, 2007) – such as in the choice and application of motors with programmable features and the application of sensors and data acquisition methods.

The Geopyörä prototype device was manufactured entirely in-house at the University of Oulu. A steel plate frame was used to avoid intricate machining operations and complicated joint pieces, with the objective of producing a machine that is light enough for laboratory use and reasonably simple to manufacture. The sensing and data acquisition systems were adapted from equipment available at the university or easy to procure.

The actual performance of the Geopyörä device was evaluated by

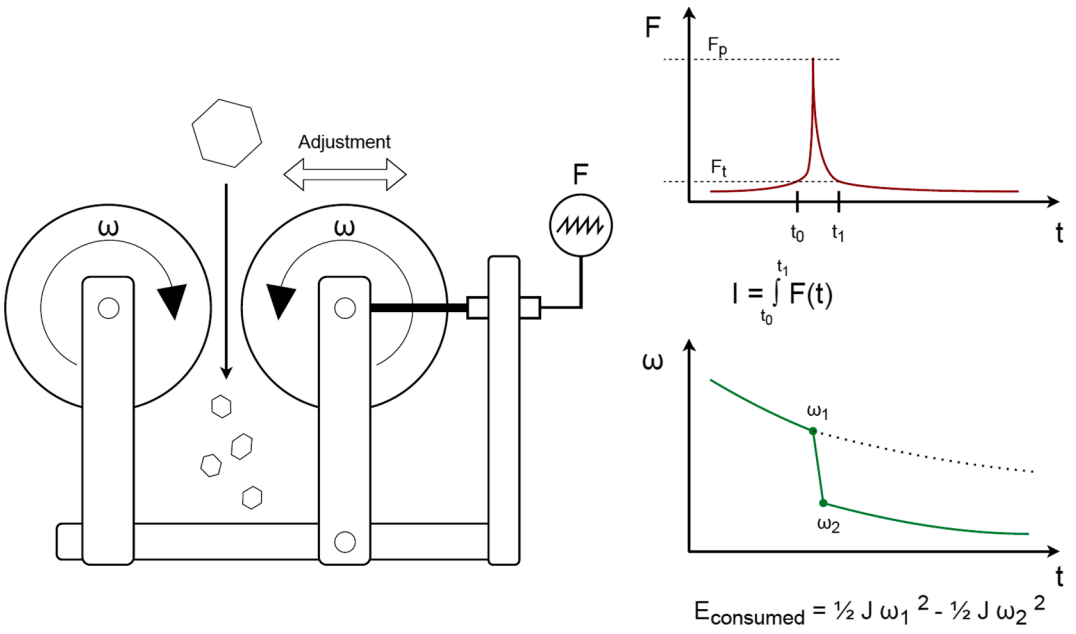

Fig. 1. Double wheel breakage test concept.

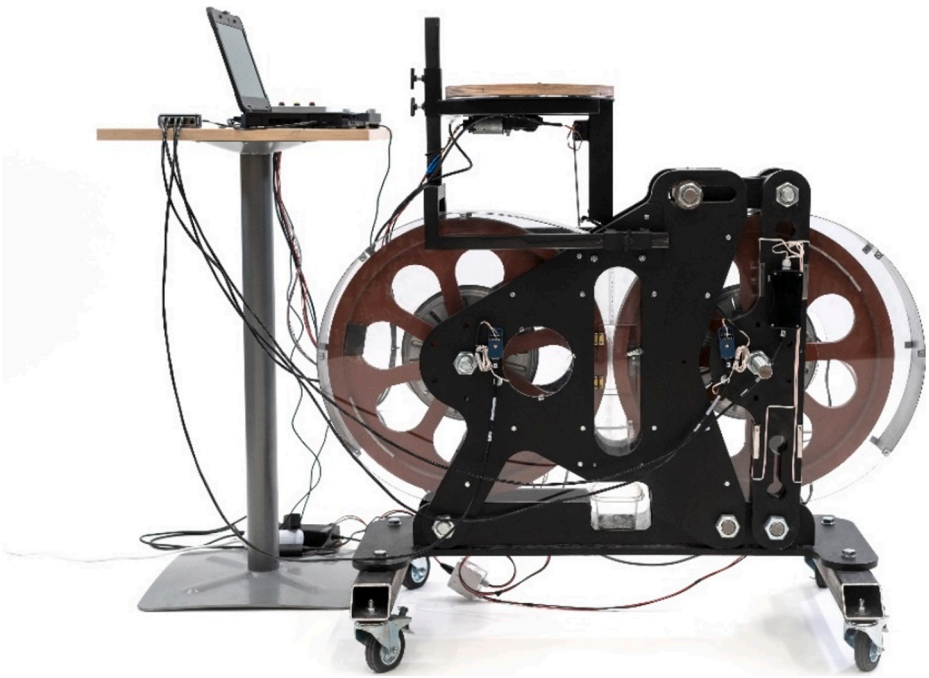

Fig. 2. Geopyörä breakage test prototype.

means of comparison against the JKDWT and SMC test, which are considered the industry standard in terms of single particle breakage test. The trials were conducted using samples from five different mines and the comparisons were done both in terms of the measured t_{10} as well as the fitted parameters A and b of the breakage Eq. (1).

The structure of the new device was proposed as a variation of a roll crusher, consisting of two counter-rotating narrow wheels with an adjustable gap and instrumentation to capture the breakage data. To design such a device, it is necessary to estimate some basic properties of the rock materials. The strength of typical rocks varies all the way from a low 3 MPa for the softest materials to a high of 464 MPa for some of the hardest rock types found in mines. The compressive or tensile strength also varies by the relative speed of deformation, known as strain rate. The highest strength is found under the very lowest and highest strain rates, under compression instead of tension. (Grady & Lipkin, 1980, Liu & Xu, 2013, Zhang, 2004, Altindag & Guney, 2010). A single particle crushing event inside a double roll crusher takes on the order of 20–35 ms (Lieberwirth et al., 2017), which translates to a relatively modest average strain rates in the magnitude of 10 s^{-1}. A non-comprehensive listing of the strengths of various rock materials under strain rates ranging between approximately 5–50,000 s^{-1} at fracture can be seen in Table 1.

Crushing a particle more rapidly to apply a higher strain rate causes more energy to be absorbed into branching fractures, secondary cracking, and micro-cracking. This leads to the rock breaking into smaller particles. At the same time, the non-absorbed energy is consumed in the kinetic energy of the resulting breakage products, friction, heat, noise, et cetera resulting in lower efficiency for the process (Zhang et al., 2000). The main reason for this inefficiency is in the random distribution of forces on the particles inside the crusher. With certain simplifications, the theoretical energy efficiency of comminution can be estimated to fall between 5 and 10 % (Legendre & Zevenhoven, 2014) while the measured energy efficiency in actual comminution testing may reach 5–14% with 6.3–141 Joules of energy applied to the samples (Zhang et al., 2000) The absolute energy consumption may reach 410 Joules for a large 60 mm sphere of rock (Refahi et al., 2010). Extrapolating by the volume of the material being crushed, a 30 mm spherical particle could require 51 Joules to crush while a 50 mm spherical particle might require up to 237 Joules. Knowing that the double roll crusher won't apply extremely high or low strain rates to the particle, one may reasonably choose that a particle of hard rock can withstand 100 MPa of stress and require between 50 and 250 Joules of energy to break depending on its size. This rationale served as the basis for defining the main design criteria.

The main technical criteria for the prototype are listed in Table 2. The basic operating procedure comprises of preparing 20–30 particles, adjusting the running speed and the gap opening of the machine, then feeding the particles through one by one. The comminution energy is adjusted by varying the size of the gap relative to the particle. The breakage product is collected from a tray underneath the machine for

Table 1
Amount of stress to fracture rock.

10–125 MPa (Grady & Lipkin, 1980)
3–60 MPa (Zhang, 2004)
7.5–110 MPa (Yan et al., 2012)
5.6–142 MPa (Whittles et al., 2006)
6.62–60.22 MPa (Liu & Xu, 2013)

Table 2
Design criteria.

Criterion	Value	Notes
Particle size range	16–50 mm	Main interest: 20–30 mm
Maximum reduction ratio	4:1	
Gap adjustment range	4–50 mm	Technically 0–50 mm
Energy output	100–250 J	
Feed rate	5–10 s per particle	
Peak loading	70 kN	30 mm spherical particle; 100 MPa strength
Highest average power demand	50 W	250 Joules every 5 s
Peak estimated power output	12.5 kW	250 Joules over 20 ms
Maximum roll surface speed	3.0 m/s	95 RPM for a roll of 600 mm in diameter
Roll diameter	600 mm	20–30 mm particle size; μ=0.24; See text.

further analysis.

The diameter of the crushing wheel depends mainly on the geometry of the particles. If the particle is too large compared to the wheel, the resultant force pushing the particle out exceeds the force of friction pulling the particle into the gap. The maximum equivalent feed particle size d can be calculated in relation to the wheel diameter DW, the gap separation s, and the coefficient of friction μ, by the Eqs. (2) and (3): (Lieberwirth et al., 2017)

$$d < (D_W + s)\sqrt{1+\mu^2} - D_W \tag{2}$$

Re-arranging for D_w:

$$D_W > \frac{d - s\sqrt{1+\mu^2}}{\sqrt{1+\mu^2} - 1} \tag{3}$$

With irregularly shaped particles of varying composition, it is impossible to give a precise coefficient of friction for the calculation. The surface speed also affects the friction between the particle and the wheels with greater speed resulting in worse nipping behaviour (Lieberwirth et al., 2017). A wheel diameter of 600 mm was chosen as a compromise to keep the machine reasonably small.

The heavy wheels were designed to store enough kinetic energy in rotation to provide the peak power output, which eliminates the need for powerful motors and permits the use of gearless low voltage DC motors. The prototype utilizes modified direct drive motors of a washing machine, running at low power from an AC-DC wall adapter. This contactless drive lets the wheels spin freely when the motor is powered off, eliminating interference from gears, chains or belts. This means the wheel system can be regarded as simple spinning masses. The motors do produce some magnetic drag along with the inherent rolling friction of the wheel bearings, which need to be compensated for in the energy estimation. One full wheel and motor assembly has a mass of approximately 52 kg, providing a combined 258 Joules of kinetic energy at 90 RPM from two wheels. The combined mechanical power output of the two motors was estimated to be 72 Watts at 60 RPM with a top speed of 121 RPM under no load. The highest stable speed with the added rolling friction of the wheels was reduced to just under 90 RPM by the limited capacity of the motor controllers used in the device. The wheels are supported by heavy roller bearings and centred axially between fixed ends stops by the magnetic attraction of the motors.

The choice of wheel material became a choice between hardness and toughness: high hardness in steel is a compromise with low impact resistance. A steel with a hardness of 400 HB may withstand an impact of 170 J/cm^2 at room temperature, while a harder steel of 700 HB may withstand less than 80 J/cm^2 (Mazur & Mikova, 2016) which would risk fracturing the wheel surfaces. The choice was made to use a common wear-resistant Raex® 450 steel with a hardness between 420 and 500 HB. The frame was built out of regular S355 carbon steel. A 3D illustration of the basic structure can be seen in Fig. 3. The device fits in a volume of approximately 140 × 50 × 90 cm and has a total mass around 225 kg before other additions.

The wheel gap adjustment mechanism consists of a pair of upright steel beams housing one of the wheels in between. The beams pivot around sleeve bearings on both ends and an adjustment link arm connects the upper end of the beam to the rest of the frame. The link arm slots between the frame in a pin-slot clamp that can be tightened by hand, allowing the wheel gap to be adjusted between 0 and 50 mm. The upright beams were instrumented with strain gauge strips to measure the amount of their bending, turning the structure into an integrated load cell. Both wheel hubs were fitted with patterned encoders and infrared optical gates as tachometers to measure the wheel speeds. A single four input strain gauge bridge measurement module from National Instruments was adapted to measure both load beams and both tachometers. Using a single data acquisition module for all sensors allowed easy and simple synchronization of the data in the measurement software. A listing of the sensing hardware used can be found in Table 3.

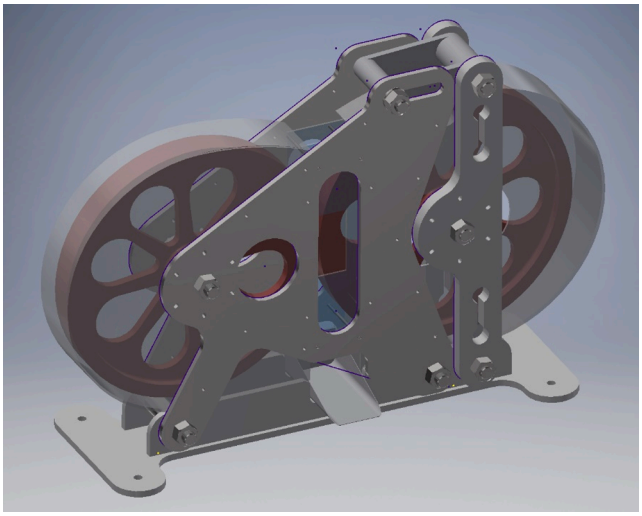

Fig. 3. 3D concept model of the Geopyörä testing device.

Table 3
Sensors and data acquisition hardware.

Part	Material	Notes
Module carrier:	cDAQ-9171	USB 2.0
Strain gauge ADC module	NI 9237	Four channel, 50 kS/s, 24-bit, full bridge
4x Screw terminals	NI 9949	RJ-50 to screw terminal adapter
4x RJ-50 cable	twisted pair cable	
2x Infrared optical gate	TCST1103	Diode and phototransistor with filter
2x Encoder wheels	1 mm fine plywood	Laser cut and painted black
8x Strain gauges	KFG-5-120-C1-11L3M3R	120 Ohm Kyowa strain gauge for steel

A stand-alone application program for using the crusher in a laboratory setting was developed with the National Instruments LabVIEW 2016 Professional software suite. The application program allows the user to monitor the crusher while adjusting the recording parameters, and automatically record and tabulate measurements.

A test is conducted by holding a rock particle ready at a predetermined height above the wheel gap, then switching both wheel motors off while immediately dropping the particle between the gap. Once the particle has passed through, the user waits a a brief moment for the measurement recording to complete and switches the motors back on. The software indicates when the wheels are running at the correct speed and the measurement can be repeated. When using the recording function, the software measures all input channels continuously. When a force event is detected, it calculates the difference in wheel speeds at particle entry and exit, converting the data to a difference in stored kinetic energy. While the first tests using the prototype were completed with manual operation, the motor controllers provide an electrical interface to automate the entire process in later versions. Once enough data has been gathered, the operator can stop the recording function and save the resulting data table. A screen capture of the application running can be seen in Fig. 4.

4. Principle of operation

The operation of the Geopyörä testing device differs from the traditional ore characterisation testing devices. As described in Table 4, unlike the traditional drop-weight-type devices (JKDWT, SMC, UFLC, HIT), the Geopyörä uses two instrumented counter-rotating wheels to measure the absorbed energies. For the JKDWT, SMC and HIT devices, energy input is calculated per size-class and assumed that all imparted drop-

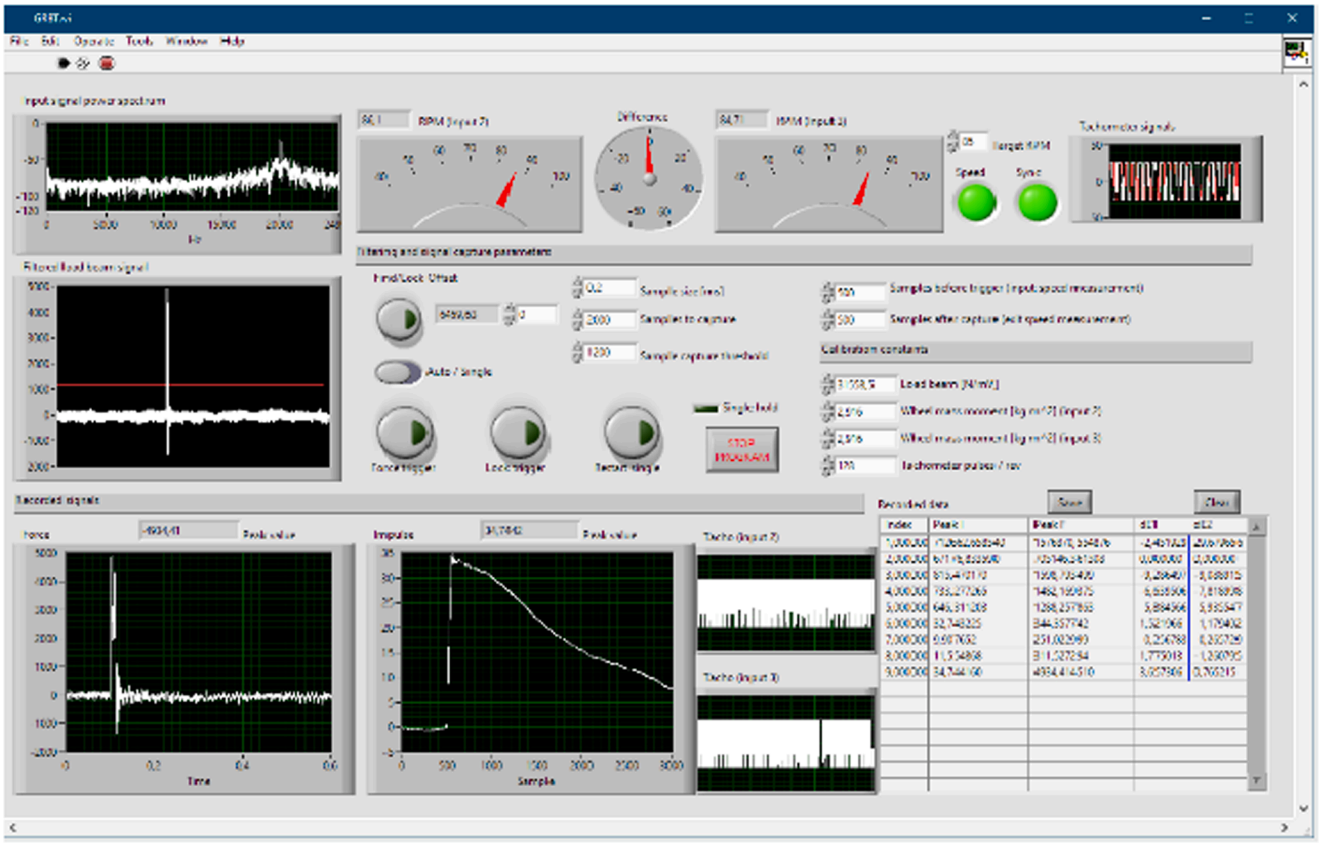

Fig. 4. Screen capture of the data recording software.

Table 4
Breakage tests comparison.

	JKDWT	SMC	UFLC	HIT Tester	Geopyörä
Developers	JKTech (1992)	Morrell (2004)	Tavares and King (1998)	Kojovic (2016)	
Energy input mechanism	Mass dropped from a height	Mass dropped from a height	Mass dropped from a height	Mass dropped from a height	Counter-rotating wheels with a controlled gap setting
Energy applied for breakage	Known mass + adjusted height to achieve calculated specific energy particle size-class	Known mass + adjusted height to achieve calculated specific energy particle size-class	Known mass + adjusted height to achieve calculated specific energy particle size-class	Known mass + adjusted height to achieve calculated specific energy particle size-class	Adjustable gap setting between rolls per particle size-class
Energy absorbed for breakage	Not measured - Assumed all drop weight energy goes into particle breakage	Not measured - Assumed all drop weight energy goes into particle breakage	Measured using high strain rate load cells	Not measured - Assumed all drop weight energy goes into particle breakage	Measured by the loss of momentum of rotating wheels per gap setting per particle size-class and load cells between the
Accuracy of energy measurement for breakage	Calculation: drop mass and height	Calculation: drop mass and height	Direct energy measurement applied for particle breakage	Calculation: drop mass and height	Direct energy measurement applied for particle breakage
Competency & Hardness measurement	JK Axb	DWI	Peak Force	Axb	Geo Axb, BWI, Peak Force
Relative testing speed per 100 rock particles per energy class	Slow	Slow	Very slow	Fast	Very fast
Likelihood of secondary breakage	High	High	Low	Low	Very low

weight energy is absorbed for particle impact breakage. Only in the UFLC device, the energy absorbed for single-particle breakage is measured using the high-strain-rate load cells. Additionally, unlike all conventional drop-weight-type devices, the testing speed of the Geopyörä is relatively fast due to the online energy logging per particle per breakage event. The online energy measurement lessens the time spent adjusting the drop height required per particle mass for the necessary specific energy in the drop-weight-type devices.

In an in-depth study undertaken by Chandramohan (2013) on the drop weight tester performance showed that the anvil's shape could bias the competency measurement, which is especially profound for the softer ores. Tests that use the drop weight devices at high energy levels (JKDWT and SMC) are likely to bias the competency measurement due to the likelihood of particle secondary or compressive breakage between the crushing head/weight and the anvil. However, re-breakage is unlikely to occur in Geopyörä because the broken fragments can freely pass through the crushing wheels gap. Furthermore, abrasion or attrition-type breakage events are minimised with the relative velocities of the dropped particles and rotational speeds matched at the nipping point.

Confirmation of a single breakage event (i.e., no re-breakage) of a rock particle is shown as a series of photographs taken with a Sony Cyber-shot DSC-RX100 IV camera (Fig. 5). The individual frames were shot through an open access hatch on the side of the device, then cropped and combined into a single image. The series shows the particle breaking into two distinct parts, with the daughter particles ejecting through the gap as a spray of dust and fragments below. Larger daughter fragments left behind do break again as they cannot pass the gap without further reduction in size, but all energy input is accounted for, while particles smaller than the gap size are not likely to break any further. In a drop weight device, both larger and smaller fragments can be compressed against the anvil and be broken further, which does not happen with Geopyörä, since the smaller fragments are able to clear the crushing zone. All energy spent on breakage is recorded as long as the fragments pass through the gap within the measurement time interval.

With the simplicity of the Geopyörä design and operation, the equipment lends itself to higher degrees of automation than in the prototype, which will be exploited in ongoing development.

5. Prototype tests

For the initial testing, the sampling parameters were set to trigger a detection of a breakage event at 1200 Newtons. Since the load cell data was not used for the initial proof of concept - only for triggering each measurement - the load sensors were calibrated approximately in a simple manner by pulling the wheels together with a steel cable tied to the link arm, and a digital scale suspended in between. A lower detection threshold could be used, but an intermittent source of electrical interference was found to produce false triggers occasionally. The gap size was selected to be 1/4, 2/4 and 3/4 of a nominal 20 mm particle size, for a total of 120 particles through each gap. The device was first set at 60 RPM and 114 Joules of stored energy. The first test particle failed to pass and stopped the wheels entirely, so the speed was increased to 85 RPM and 231 Joules of stored energy for all subsequent tests. After some experimentation, it was found possible to process a batch of 30 particles in under ten minutes by manually feeding the device. Fig. 6 illustrates the raw energy data measured from the initial test set. The sample values are sorted from lowest to highest measured energy consumption. Some particles passing through the largest gap did not register enough force to trigger the measurement. Most of these particles passed through with minimum or no breakage, and they are recorded as consuming zero energy in the experiment data.

After subtracting the energy used by the machine itself, the mean energy levels recorded for the different gap settings were 13,08 J, 26,31 J and 64,84 J respectively. The greatest energy consumption recorded for a single particle was just under 200 Joules not including the energy used by the device itself. This shows a clear difference in overall energy consumption between the different gap settings. Many of the particles at the largest gap opening were passing through with little or no energy consumed, barely touching the wheels because of their flattened shapes. If the shapes varied too much, the machine could not reliably break the particles at the widest gap opening. Rather than getting pulverized, the particles would split into few larger fragments that would pass the gap without further breakage. With little or no breakage products below the t_{10} level, and little to no energy recorded, these particles would effectively be treated as out layers and get excluded from the data.

The baseline energy consumption of the device itself was measured by switching the motors off at speed and manually triggering the software to record an event without a particle passing through. Closer examination of the wheel energy loss data revealed a problem in the way the program was measuring very small differences at the highest wheel speeds, causing the consumed energy measurement to quantize to increments of 6–8 Joules at the lowest energy levels. This effect is visible

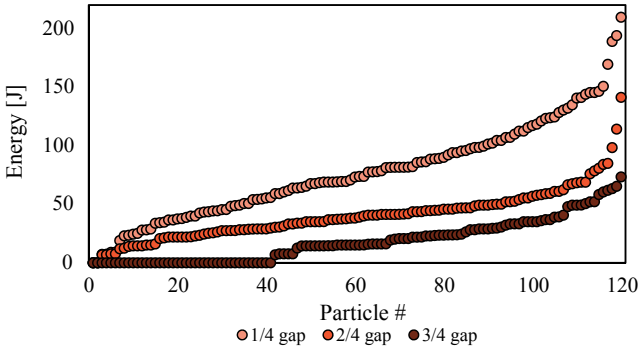

Fig. 6. Distribution of measured energy consumption at three different gap openings.

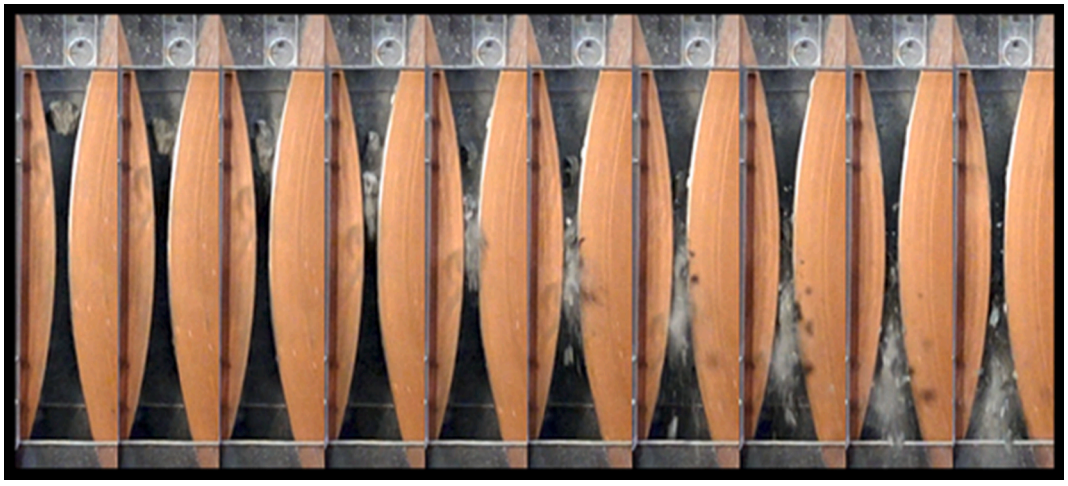

Fig. 5. A series of high-speed photographs of a typical crushing event.

in Fig. 4. in the stepwise shape of the ¾ gap energy distribution curve. The programming error was caused by a misunderstanding of the LabVIEW programming documentation and corrected for later tests. With the corrections in place, the mean no-load energy consumption at 85 RPM was measured to be 13,51 Joules with a standard deviation of 1,07 Joules – both becoming proportionally smaller at lower wheel speeds.

While the crushing load on the wheel does influence the amount of energy lost to friction in the bearings, the actual peak breaking force event was found to be practically instantaneous and the loss of energy to the operation of the machine itself is almost entirely dominated by the idle rolling friction of the wheels over the fixed time interval between the detected particle entry and exit speed measurements. To account for this, the measurement software was improved for further tests to measure the mean speed over the measurement interval and correlate this with a rolling friction model of the system which is calibrated by measuring the idle energy loss at various speeds. Subtracting the friction estimate from the measured breakage energy gives the true value of breakage energy to within the uncertainty or deviation of the measurement.

6. Preliminary breakage test results

A number of different ore samples have been tested to date in order to verify if the prototype device would be capable of detecting changes in rock competency/hardness. The greatest advantage of the new method is that it allows data to be measured and recorded as distributions, not only averaged values, which is ideal to compare samples with statistical evidence. Fig. 7 shows the Peak Force (kN), Impulse (N.s), Energy and Specific Energy (Ecs in kWh/t) as measured at the same gap ratio (1/2) for 7 different samples with 40 particles of 20 mm each. In the probability distributions graphs, presented in Fig. 7, the values plotted along the X axis are in units of standard deviation. These Normal Score values represent the z-scores from a standard normal distribution (mean = 0 and a standard deviation = 1, hence N score not Z score). Data is plotted against the normal scores from that distribution.

The natural variation in rock strength within a sample due to variations in particle shape are captured within these distributions, while DWT methods do not show this variation which is hidden or ignored. Chandramohan (2013) investigated the response of rock strength to particle shape in JKDWT results and highlighted that the competency measurement (i.e. Axb) using the standard procedure is compromised when different particle shapes are tested in different orientations. In the Geopyörä design, the applied energy for breakage can also be affected by the particle thickness between the counter-rotating wheels, but it is fairly consistent within a narrow size class due to particles self-orienting when free falling into the gap. Therefore the difference in rock hardness due to shape itself can be reduced.

The peak force (F) for fracture alone or even the measured specific comminution energy distributions (Ecs) can be a good indicators of rock strength and used to compare samples. In Fig. 8, the measured F and Ecs data for these seven ore samples are compared by means of ANOVA, which allows to easily confirm and identify the differences in rock strength across these samples.

7. Application to traditional breakage measures

Despite using a different concept, it is important for the new breakage test to be capable of accurately reproducing the results of industry standard tests. This adds great value to the new method and continuity to existing databases. Therefore, further validation of the new breakage test device was made by means of comparison trials against the JKDWT and SMC Test results using bulk samples five ores from different mine sites as listed in Table 5. The tests conditions are summarized in Table 6 and described as follows.

The JKDWT uses 15 sets of particles between the size of −63 + 53 mm to −16 + 13.2 mm while the SMC Test uses less material, with two

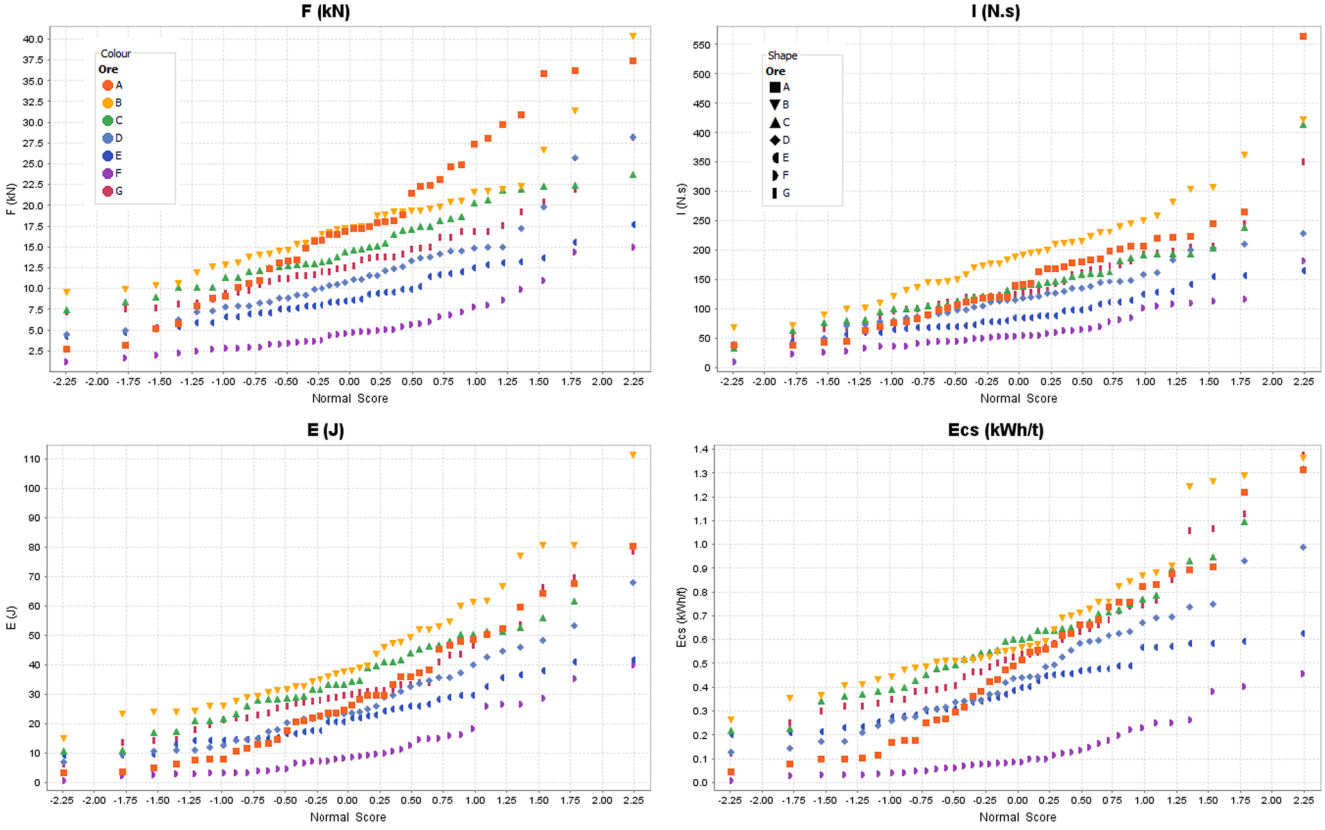

Fig. 7. Distribution of measured peak force, impulse, energy and specific energy at the same gap opening for 7 samples.

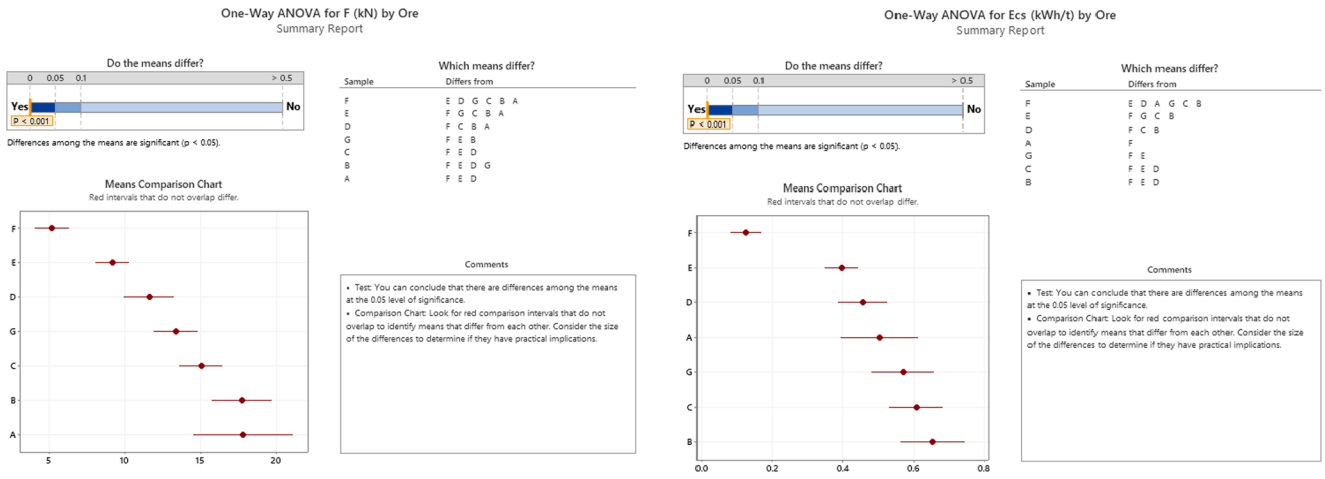

Fig. 8. ANOVA for peak force and specific energy data measured at the same gap opening for 7 samples.

Table 5
Deposit description of particle samples.

Ore	SG	Deposit type
A	2,95	Gold mine
B	3,20	Polymetallic mine
C	2,98	Nickel – Zinc mine
D	2,90	Polymetallic mine
E	2,80	Phosphate mine

Table 6
Sample preparation requirements.

Size (mm)	Drop Weight Test		SMC		Geopyörä	
	Particles	Energy	Particles	Energy	Particles	Gap
−63 + 53	10	0,4	X	X	X	X
	10	0,25				
	10	0,1				
−45 + 37,5	15	1,0	X	X	X	X
	15	0,25				
	15	0,1				
−31,5 + 26,5	30	2,5	20	1,76	X	X
	30	1,0	20	0,49		
	30	0,25	X	X		
−22,4 + 19	30	2,5	20	1,76	30	1/4
	30	1,0	20	0,49	30	2/4
	30	0,25	X	X	30	3/4
−16 + 13,2	30	2,5	X	X	X	X
	30	1,0				
	30	0,25				

samples sets of 20 particles in the size range of −31.5 + 26.5 mm to −16 + 13.2 mm. For the Geopyörä test, after the preliminary evaluation of the prototype performance, the particle size selected was −22.4 + 19 mm. Both JKDWT and SMC Test use pre-determined energy levels, while the Geopyörä test has variable energy levels which can be adjusted by changing the gap aperture. The energy range for the JKDWT test is between 0.1 kWh/t to 2.5 kWh/t while the SMC Test used two energy levels of 1.76 kWh/t and 0.49 kWh/t. The Geopyörä test was set up with three gap sizes at 1/4, 2/4 and 3/4 of the particle geometric mean, which represent high and low energy levels respectively.

The three sets of 30 particles for the Geopyörä tests were selected with the same methodology used in the JKDWT (i.e. randomly selected). The samples for JKDWT and SMC Test were prepared according to the criteria of the presented in Table 5 and sent to the Wardell Armstrong laboratory in the UK, where the standard tests were performed. The resulting A and b parameters as reported by JKTech Pty are listed in Table 7.

The A and b parameters describe the behaviour of the t_{10} – Ecs curve described in Eq. (1) wherein t_{10} is defined as the percentage of material which passes under one-tenth of the size of the original particle. While the Axb parameter represents the ore resistance to breakage, with lower values meaning more competent rock.

The validation of the Geopyörä tests presented in this paper measures the total specific energy as an average of each breakage event as shown in Eq. (4). Where the variables E_1 and E_2 represent the energy consumption recorded by each wheel in Joules, F is the measured energy loss due to friction and magnetic drag in Joules, n is the number of particles in the sample, and M is the sample mass in kilograms. The constant coefficient 1/3.6 is a conversion factor between Joules per kilogram to kilowatt-hours per ton. A single fixed value for F was used for all tests as measured previously.

$$Ecs = \left[\frac{\left(\frac{E_1+E_2}{n}\right) - F}{\frac{M}{n}}\right] \cdot \frac{1}{3.6} \tag{4}$$

The energy values obtained in each test are presented in Table 7. Since these values do not match the JKDWT and SMC Test standard energy levels, it is not possible to directly compare their measured t_{10} against those obtained with the Geopyörä. Therefore, the reported A and b values for both JKDWT and SMC Test were used in breakage Eq. (1) to calculate an apparent t_{10} at the energy levels as measured by the Geopyörä in order to compare them. The result of this t_{10} comparison is shown in Table 8 as well as in Fig. 9.

Additionally, the A and b parameters for Geopyörä tests were fitted using the measured specific energy and t_{10} values as listed in Table 7. The resulting A, b, and Axb parameters for the Geopyörä tests are listed in Table 9. The comparison of Axb values obtained with the Geopyörä versus those measured by the JKDWT and SMC Test is shown in Fig. 10.

Although the Geopyörä tests used only one particle size and three

Table 7
Axb results reported in the JKDWT and SMC tests.

Ore	JKDWT			SMC		
	A	b	A × b	A	b	A × b
A	57,9	0,55	31,8	72,7	0,41	29,8
B	71,2	0,49	34,9	81,9	0,44	36,0
C	78,3	0,40	31,3	100	0,30	30,0
D	67,6	0,89	60,2	72,7	0,85	61,8
E	67,8	1,31	88,8	66,2	1,44	95,3

Table 8
Comparison of the calculated JKDWT and SMC t_{10} and the measured t10 of Geopyörä test.

Ore	Ecs (kW/t)	DWT t10 (%)	SMC t10 (%)	Geopyörä t10 (%)
A	0,95	23,5	23,4	26,7
	0,52	14,5	14,0	15,7
	0,25	7,6	7,2	4,1
B	1,21	31,9	33,9	32,8
	0,42	13,3	13,8	11,5
	0,24	7,9	8,2	5,2
C	1,18	29,4	29,7	29,1
	0,47	13,3	13,0	11,2
	0,04	1,3	1,3	1,0
D	0,71	31,7	32,9	33,5
	0,36	18,7	19,3	16,2
	0,11	6,3	6,5	5,6
E	1,15	52,8	53,6	51,5
	0,44	29,6	30,9	29,6
	0,29	21,6	22,7	18,7

energy levels, which cannot be precisely selected and do not reach very high levels as in the JKDWT or SMC Tests, the obtained Axb and t_{10} parameters for all samples were in good agreement with the standard tests results. The only minor discrepancies were seen in the model fitted for ore types A and D, as shown in Fig. 11, but it did not cause any significant bias in the calculated Axb.

8. Application to future ore body characterisation

As can be deduced from the different breakage method and integrated instrumentation, this new testing technique opens up new avenues to characterising rocks and ore bodies for mining. Particular capabilities are:

- Providing a distribution of particle strength given by both the absorbed energy and reaction force of the compressing wheels
- The prospect of automating the gap to provide a precise reduction ratio for rocks of different feed size ranges and of different geometries (flakiness)
- Online single particle size/shape/volume analyser using image, contour, or laser analysers, providing also online density distribution measurement if combined with a continuous single particle scale.
- Online multi-component product size distribution data using coloured image analysis.

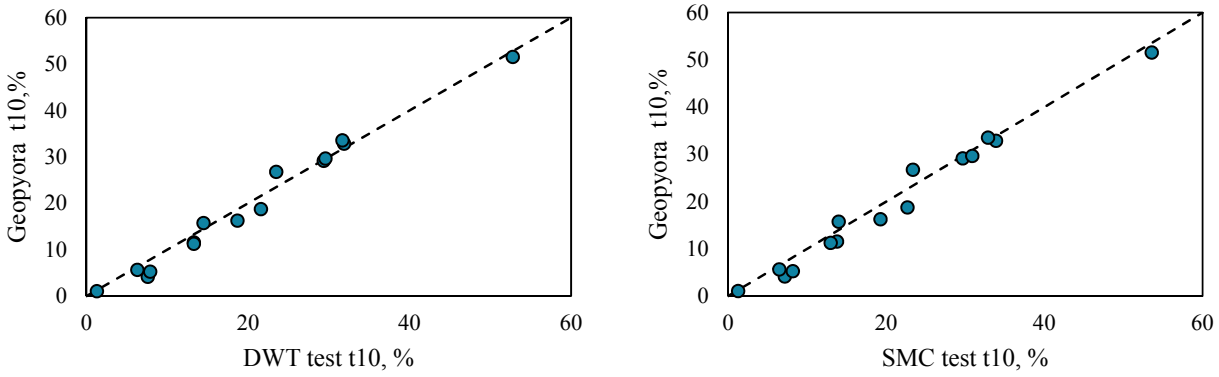

Fig. 9. Comparison of t_{10} values between the Geopyörä test and the DWT test, SMC test.

Table 9
Axb results for the Geopyörä test.

Ore	A	b	A × b
A	*100*	*0,33*	*32,8*
B	*100*	*0,32*	*32,1*
C	*100*	*0,29*	*28,5*
D	*100*	*0,55*	*55,0*
E	*63,7*	*1,43*	*91,2*

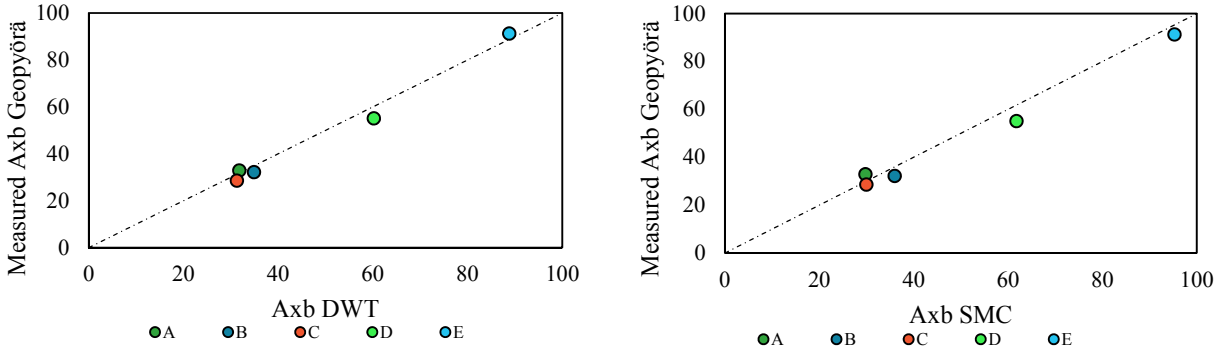

Fig. 10. Comparison of Axb values of the Geopyörä test against the DWT test, SMC test.

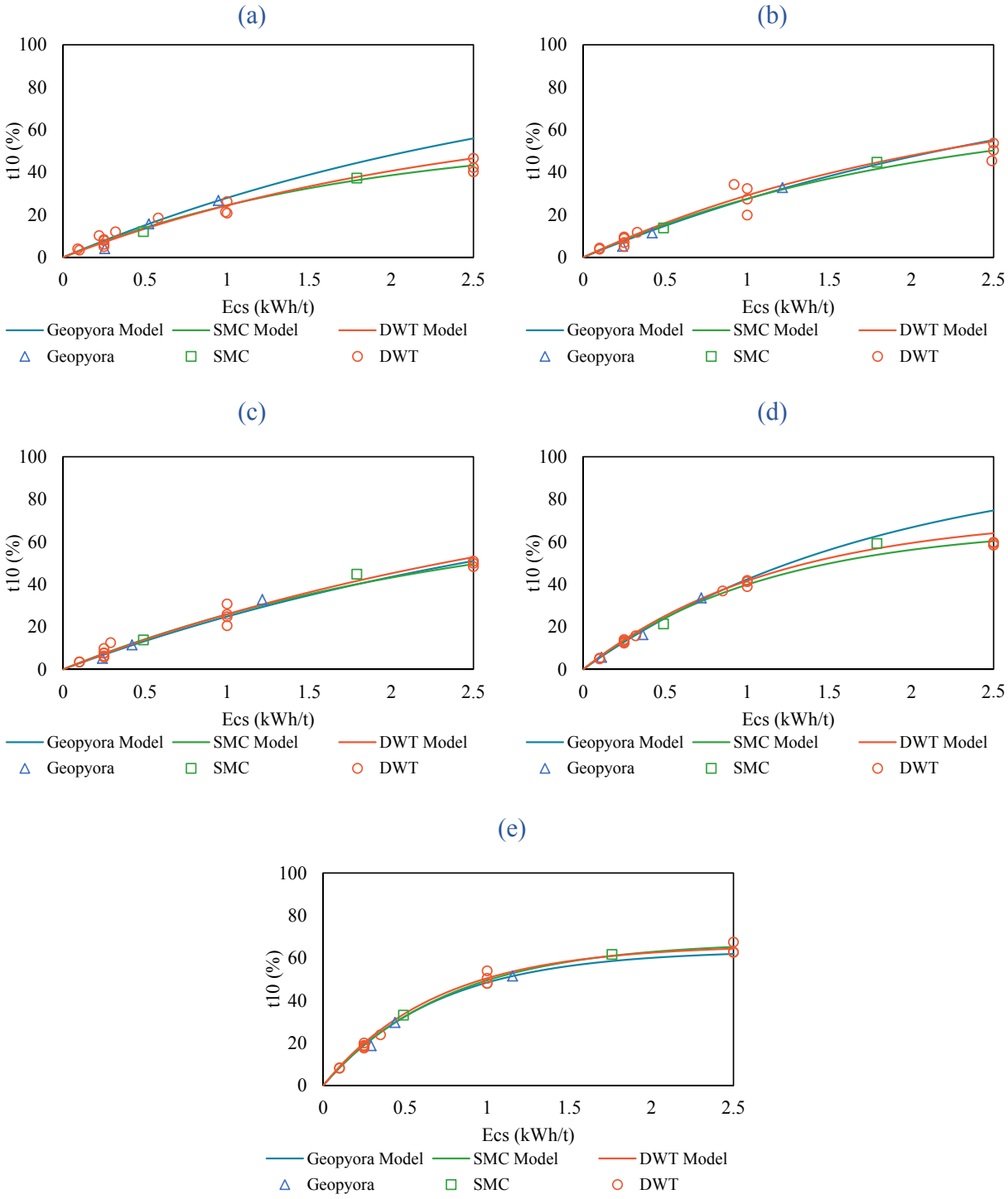

Fig. 11. Ecs vs t10 curve for (a) Mine A, (b) Mine B, (c) Mine C, (d) Mine D, (e) Mine E.

- Online texture/composition of particles using image analysis or even tomography (if technology is available).
- Automated feeder. Crushed rocked particles are fed into a bin, where particles are separated by a vibrating hopper and belt feeder. The idea here is to separate the particles individually, such that they can be fed into the breakage tester one rock particle at a time.
- Rotation of Flaky shapes. A chute design that changes the directional flow of flaky particles can be incorporated into the design of Geopyörä. This design provides a distribution of hardness for varying shapes (Chandramohan, 2013).
- In case of automation of one feed size at a time. Use Kason screen or similar type of device for online feed screening.

These capabilities open up a range of additional ore measures for no extra cost or testing time. Thus the value of the Geopyörä is not in just being a more rapid and lower cost test to replace traditional DWT methods, but in extending the outputs to allow for more advanced ore body modelling and for use in advancing mechanistic equipment models, such as those of de Carvalho and Tavares (2013) or proposed by Powell (2018, 2006).

The distribution of competence within a sample will be routinely

provided, with force to fracture adding a measure of compressive strength significant to rock mechanics and crushing. Such measures have been exceedingly tedious to measure with current fast loadcell devices, which has precluded then from common use in process modelling and ore body characterisation, but this is overcome with the new rapid measures of the Geopyörä. This opens up the door to improved methods of Geomet modelling, such as proposed by Powell (2013) and demonstrated as viable by Yildirim et al (2014).

9. Conclusions and discussion

The data collected with the device shows measurable differences between the consumed energy levels at different gap settings. While the energy level cannot be controlled as precisely as in the JK Drop Weight Test, it can be varied to produce different levels of breakage which is necessary for fitting the parameters of the breakage curve in Eq. (1). Instead of applying a nominal amount of energy, the device is measuring the actual applied energy. The main limitation of this technique is the estimation of energy loss due to friction and magnetic drag, which in the initial version of the test was calibrated once and considered a constant. The observed 1.07 Joule random deviation should be considered the technical precision or uncertainty of the prototype machine under the applied testing parameters, while the accuracy of the estimate depends on correctly identifying the amount of energy used to rotate the wheels themselves.

After accounting for the energy used by the machine itself, some residual error is expected because the assumption of a constant amount is not correct. The amount of rolling friction in the wheels can however be measured at various running speeds, and the remaining error can be compensated for by observing the actual speeds of the wheels during a breakage event. This is done automatically in the improved versions of the test. In addition, the impulse of force during the crushing event could be used to estimate the wheel loading for a secondary correction factor to further refine the accuracy of the estimate. Better characterization of the load beam behaviour will enable additional features such as the simultaneous estimation of the compressive strength of the particles in future versions of the test.

The device is reasonably quick to operate. The present means of using optical encoders and measuring a difference in stored kinetic energy before and after particle breakage is fundamentally sound, but the implementation needs refinement. Finer construction of the wheels and wheel speed encoders will improve the results. Since the particle and all fragments pass through the gap only once and do not compress into one another afterwards, there is no secondary re-breakage of daughter particles into finer particles to distort the resulting t_{10}, avoiding some of the potential issues present in some of the existing comminution tests. However, in its current form, the device is not able to apply as much specific energy to the samples. In comparison to the commercial JKDWT and SMC Test performed, the Geopyörä device shows good agreement in the measured values. Since the accuracy of these individual test cases is unknown, this initial evaluation cannot establish exact limits for the accuracy of the Geopyörä device and this should be a topic for further research.

This work was conducted to design, build and test a functioning prototype device for measuring the comminution of rock particles. Based on the measurements and data collected on so far, the device meets its basic requirements and specifications regardless of some minor issues. It has the potential to be improved for greater accuracy and precision with further refinement of both hardware and software.

Credit authorship contribution statement

Marcos Bueno: Conceptualization, Supervision, Writing - review & editing, Funding acquisition, Project administration. **Janne Torvela:** Writing - original draft, Methodology, Resources, Investigation, Software. **Rajiv Chandramohan:** Conceptualization, Review and editing. **Tabatha Chavez Matus:** Formal analysis, Investigation, Writing. **Toni Liedes:** Supervision, Project administration. **Malcolm Powell:** Project advisor, Review and editing.

Declaration of Competing Interest

The authors declare that they have no known competing financial interests or personal relationships that could have appeared to influence the work reported in this paper.

Acknowledgements

This work was supported by the Business Finland public agency for research funding. The prototype machine was constructed and tested as a collaboration between the Intelligent Machines and Systems research unit and the Oulu Mining School at the University of Oulu. We thank everyone involved in providing the experimental materials and data, and our supporters for making this work possible. We express our gratitude to all our colleagues for sharing their help and expertise, and to the university for the opportunity to perform this research and publish the results.

Appendix A. Supplementary material

Supplementary data to this article can be found online at https://doi.org/10.1016/j.mineng.2021.106905.

References

Acar, M., Parkin, R.M., 1996. Engineering education for mechatronics. IEEE Trans. Ind. Electron. 43 (1), 106–112.
Altindag, R., Guney, A., 2010. Predicting the relationships between brittleness and mechanical properties (UCS, TS and SH) of rocks. 5(16), 2107–2118.
Bourgeois F., K. R. P. and H. J., 1992. Low-impact-energy single particle fracture. In: Kawatra, S.K. (Ed.), Comminution: Theory and practice, pp. 99–108.
Bueno, M., Foggiato, B., Lane, G., 2015. Geometallurgy applied in comminution to minimize design risks. SAG Conference.
Cetinkunt, S., 2007. Mechatronics. John Wiley.
Chandramohan, R., 2013. PhD Thesis - Effect of Particle Shape in Comminution. University of Queensland, Australia.
Chandramohan, R., Lane, G., Foggiatto, B., Bueno, M., 2015. Reliability of some ore characterization tests. SAG Conference. https://www.researchgate.net/publication/323218453.
de Carvalho, R.M., Tavares, L.M., 2013. Predicting the effect of operating and design variables on breakage rates using the mechanistic ball mill model. Miner. Eng. 43–44, 91–101.
Grady, D.E., Lipkin, J., 1980. Criteria for impulsive rock fracture. Geophys. Res. Lett. 7 (4), 255–258. https://doi.org/10.1029/GL007i004p00255.
Hsu, T.R., 1997. Mechatronics - an overview. IEEE Trans. Compon., Packaging Manuf. Technol.. Part C. Manuf. 20 (1), 4–7. https://doi.org/10.1109/3476.585138.
JKDWT, 1992. Developed by Dough Brown - JKTech Internal Report.
Kojovic, T., 2016. HIT - a Portable Field Device for Rapid Testing at Site. AUSIMM Mill Operators Conference 2016.
Legendre, D., Zevenhoven, R., 2014. Assessing the energy efficiency of a jaw crusher. Energy 74 (C), 119–130. https://doi.org/10.1016/j.energy.2014.04.036.
Lieberwirth, H., Hillmann, P., Hesse, M., 2017. Dynamics in double roll crushers. Miner. Eng. 103–104, 60–66. https://doi.org/10.1016/j.mineng.2016.08.009.
Liu, S., Xu, J., 2013. Study on dynamic characteristics of marble under impact loading and high temperature. Int. J. Rock Mech. Min. Sci. 62, 51–58. https://doi.org/10.1016/j.ijrmms.2013.03.014.
Mazur, M., Mikova, K., 2016. Impact resistance of high strength steels. Mater. Today:. Proc. 3 (4), 1060–1063. https://doi.org/10.1016/j.matpr.2016.03.048.
Morrell, S., 2004. Predicting the specific energy of autogenous and semi-autogenous mills from small diameter drill core samples. Miner. Eng. 17 (3), 447–451. https://doi.org/10.1016/j.mineng.2003.10.019.
Morris, W., 1994. Measuring the strength of abrasive grains (Patent No. US5392633A).
Mwanga, A., Lamberg, P., Rosenkranz, J., 2015. Comminution test method using small drill core samples. Miner. Eng. 72, 129–139. https://doi.org/10.1016/j.mineng.2014.12.009.
Napier-Munn, T., Morrell, S., Morrison, R., Kojovic, T., 1996. Mineral Comminution Circuits Their operation and optimization. Julius Kruttsnitt Mineral Research Center.
Narayanan, S., Whiten, W., 1988. Determination of comminution characteristics from single particle breakage tests and its application to ball mill scale-up. (Trans. Ins).
Nogychi, T., Watanabe, M., 1992. Apparatus for measuring grindability of powder material (Patent No. US5133209A).

Powell, M.S., 2006. The Unified Comminution Model - a conceptually new model. In: Proceedings of the XXIII IMPC. 3 - 8 Sep. 2006. Istanbul, Turkey. ISBN 975-7946-27-3. pp. 1783-1788.

Powell, M.S., 2013. Utilising Orebody knowledge to improve comminution circuit design and energy utilisation. In: Proceedings of The Second AUSIMM International Geometallurgy Conference, Brisbane, QLD, 30 Sep - 2 Oct.

Powell, M.S., 2018. Developing a mechanistic mill model. Proc. Comminution 18, Cape Town, South Africa, April. publ. MEI.

Refahi, A., Aghazadeh Mohandesi, J., Rezai, B., 2010. Discrete element modeling for predicting breakage behavior and fracture energy of a single particle in a jaw crusher. Int. J. Miner. Process. 94 (1–2), 83–91. https://doi.org/10.1016/j.minpro.2009.12.002.

Tavares, L.M., King, R.P., 1998. Single particle fracture under impact loading. Int. J. Miner. Process. 54, 1–28.

Weichert, R., Herbst, J., 1986. An Ultrafast Load Cell Device for Measuring Particle Breakage. Particle Technology.

Whittles, D.N., Kingman, S., Lowndes, I., Jackson, K., 2006. Laboratory and numerical investigation into the characteristics of rock fragmentation. Miner. Eng. 19 (14), 1418–1429. https://doi.org/10.1016/j.mineng.2006.02.004.

Yan, F., Feng, X.T., Chen, R., Xia, K., Jin, C., 2012. Dynamic tensile failure of the rock interface between tuff and basalt. Rock Mech. Rock Eng. 45 (3), 341–348. https://doi.org/10.1007/s00603-011-0177-y.

Yildirim, B.G., Bradshaw, D., Powell, M.S., Evans, C., Clark, A., 2014. Development of an effective and practical Process Alteration Index (PAI) for predicting metallurgical responses of Cu porphyries. Miner. Eng. 69, 91–96.

Zhang, Z.X., 2004. Estimate of loading rate for a TBM machine based on measured cutter forces. Rock Mech. Rock Eng. 37 (3), 239–248. https://doi.org/10.1007/s00603-004-0025-4.

Zhang, Z.X., Kou, S.Q., Jiang, L.G., Lindqvist, P.A., 2000. Effects of loading rate on rock fracture: Fracture characteristics and energy partitioning. Int. J. Rock Mech. Min. Sci. 37 (5), 745–762. https://doi.org/10.1016/s1365-1609(00)00008-3.